Electronic structure and bonding of ozone

Apostolos Kalemos[a] and Aristides Mavridis[b]
Laboratory of Physical Chemistry, Department of Chemistry, National and Kapodistrian University of Athens, P.O. Box 64 004, Zografou, Athens 157 10, Greece

(Received 27 March 2008; accepted 26 June 2008; published online 6 August 2008)

The ground and low-lying states of ozone (O_3) have been studied by multireference variational methods and large basis sets. We have constructed potential energy curves along the bending coordinate for $(1,2)\ ^1A'$, $(1,2)\ ^1A''$, $(1,2)\ ^3A'$, and $(1,2)\ ^3A''$ symmetries, optimizing at the same time the symmetric stretching coordinate. Thirteen minima have been located whose geometrical and energetic characteristics are in very good agreement with existing experimental data. Special emphasis has been given to the interpretation of the chemical bond through valence-bond-Lewis diagrams; their appropriate use captures admirably the bonding nature of the O_3 molecule. The biradical character of its ground state, adopted long ago by the scientific community, does not follow from a careful analysis of its wave function. © *2008 American Institute of Physics*.
[DOI: 10.1063/1.2960629]

I. INTRODUCTION

The ozone molecule (O_3) can be thought of as a triatomic allotrope of dioxygen (O_2). It is well known by now that it is diamagnetic, thermodynamically unstable with respect to O_2, and has a v-shaped geometry with an $\measuredangle$OOO angle $\theta_e=116.7542\pm0.0025°$ and a bond distance $r_e=1.272\ 76\pm0.000\ 15$ Å, as obtained from high resolution infrared spectra.[1] It is fair to mention, however, that the first, in essence, definitive geometry of O_3 was obtained as early as 1953 by Trambarulo *et al.*[2] through microwave spectroscopy. These workers obtained $r_e=1.278\pm0.003$ Å, $\theta_e=116.82\pm0.50°$, and a dipole moment $\mu=0.53\pm0.02$ D. The most accurate experimental dipole moment recorded so far is $\mu=0.533\ 747(3)$ D.[3]

A very large number of experimental and theoretical studies have been devoted to the low-lying states of O_3. The interest on ozone was increased dramatically after the paper by Molina and Rowland in 1974,[4] referring to its interaction with man-made chlorofluorocarbons and its subsequent depletion in stratosphere, resulting in turn to the diminishing shielding of the Earth's inhabitants from the ultraviolet radiation due to the strong O_3 absorption between 220 and 290 cm^{-1} (Hartley band).

The electronic structure of O_3 has been the subject of a plethora of theoretical studies, starting mainly in the early 1970s.[5–7] Nevertheless, it does not seem to exist a recent, systematic, and comprehensive high level study of the ground and low-lying states of O_3, focusing on its electronic structure and bonding through the construction of potential energy profiles (PEPs) and with no symmetry constraints other than C_s. On the other hand, the remarkable work of Schinke's group extending to 39 publications starting in 1997, centers, primarily, on the O_3 dynamics and spectroscopy.[8]

The authors of the earliest group,[5] employed generalized valence bond (GVB)+configuration interaction (CISD) calculations coupled with $[4s2p]$ or $[3s2p1d]$ basis sets, to study the ground and a series of excited states, spanning an energy range of 5.5 eV. In the introduction of Ref. 5(d) it is stated that, "These studies showed that the ground state of ozone is well represented as a biradical

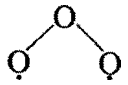

with weak bonding between the singly occupied π orbitals on the terminal oxygen atoms." This view, i.e., the biradical character of the ground state of O_3, has been well accepted from the scientific community and holds good up to these days.[7(b),7(c),9–14] However, our variational multireference calculations do not show a biradical character, or at least, the consistent interpretation of our results do not need to invoke any open singlet biradical interpretation (*vide infra*).

The Peyerimhoff group[6] performed MRD-CI calculations (multireference+selected singles and doublets +extrapolation), using $6s4p1d$ contracted Gaussian basis sets augmented by a set of s or s and p bond-type functions located between the oxygen atoms of O_3. In these series of papers the authors have calculated potential energy surfaces (PES) and potential energy profiles (PEP) of the ground and certain excited states, transition moments, and dissociation energies, aiming, mainly, in interpreting the experimental spectroscopy of ozone.

Relevant results from the collection of papers given in Ref. 7 will be discussed later on in the present work.

The motivation of the present study is the examination of the ground and a series of excited states, specifically stationary states located on optimized PEPs of symmetries $^{1,3}A'$ and $^{1,3}A''$. We employ quantitative basis sets, multireference variational methods (internally contracted MRCI=CASSCF +single+double replacements), and we have constructed PEPs with respect to the $\measuredangle$OOO$(=\theta)$ angle ranging from

[a]Electronic mail: kalemos@chem.uoa.gr.
[b]Electronic mail: mavridis@chem.uoa.gr.

TABLE I. Total energies $E(E_h)$, geometries r_e(Å), θ_e (degrees), dipole moments $\mu_e(D)$, separation energies $T_e(\mathrm{cm}^{-1})$, and barrier to linearity BL(kcal/mol) of 13 states at the MRCI(MRCI+Q)/4Z level.

State[a]	$-E$	r_e	θ_e	μ_e	T_e	BL
$\tilde{X}\ ^1A'_G(\tilde{X}\ ^1A_1)$	225.142 16	1.2724	116.82	0.546	0.0	88.8 to $^1\Delta_g$
	(225.1959)	(1.277)	(116.75)			(85.7)
Expt		1.272 76(15) [b]	116.7542(25)[b]	0.533 747(3) [c]		
$1\ ^3A''_G(^3A_2)$	225.093 67	1.3412	98.78	0.617	10 643	43.5 to $^3\Sigma^-_g$
	(225.1504)	(1.342)	(98.64)		(9968)	(41.7)
Expt		1.345[d]	98.9[d]		9963±4[e]	
$1\ ^1A'_L(^1A_1)$	225.092 51	1.4401	60.0	0.0	10 896.5	
	(225.1467)	(1.441)			(10 790)	
$1\ ^3A'_G(^3B_2)$	225.091 75	1.3542	108.55	0.197	11 063	57.6 to $^3\Pi_u$
	(225.1467)	(1.355)	(108.47)		(10 793)	(50.5)
Expt[f]					10 485	
$1\ ^1A''(^1A_2)$	225.085 14	1.3460	99.45	0.615	12 514	52.9 to $^1\Delta_g$
	(225.1413)	(1.348)	(99.04)		(11 972)	(51.3)
Expt[f]					~12 905	
$1\ ^3A''_L(^3B_1)$	225.083 59	1.3120	126.44	0.156	12 853.5	37.2 to $^3\Sigma^-_g$
	(225.1404)	(1.316)	(126.80)		(12 178)	(35.2)
Expt					11 695,[f] 11 937±242 [g]	
$2\ ^3A''_G$	225.078 21	1.3342	115	0.206	14 035.7	69.2 to $^3\Pi_u$
	(225.1349)	(1.335)	(115)		(13 385)	(43.2)
$2\ ^1A''_G$	225.066 20	1.3504	120.10	0.208	16 669.3	72.9 to $^1\Pi_u$
	(225.1231)	(1.353)	(118.0)		(15 966)	(71.0)
Expt					16 454±242 [g]	
					16 385+20 [h]	
$2\ ^1A'(^1A_1)$	225.047 33	1.3924	85.0	0.186	20 810	36.0 to $^1\Sigma^+_g$
	(225.1035)	(1.393)	(85)		(20 272)	(35.1)
$2\ ^3A'_G(^3B_2)$	225.026 79	1.4234	103.71	0.040	25 323.3	38.7 to $^3\Sigma^+_g$
	(225.0812)	(1.424)	(103.7)		(25 158)	(37.0)
$^3\Pi^i_{u,L}$	225.007 37	1.4501	180.0	0.0	29 582.3	0.0
	(225.0660)	(1.450)			(28 509)	
$2\ ^3A'_L$	224.997 00	1.4749	154.95	0.024	31 859	20.0 to $^3\Pi_g$
	(225.0557)	(1.473)	(154.4)		(30 761)	(21.0)
$2\ ^1A''_L$	224.991 97	1.7196	46.43	0.284	32 961	
	(225.0493)	(1.703)	(46.6)		(32 160)	

[a]G and L refer to global and local minima, respectively; in parenthesis C_{2v} symmetry species.
[b]Reference 1.
[c]Reference 3.
[d]Reference 17. From the analysis of the rotational structure of the high resolution FT 0^0_0 absorption spectrum of the $^3A_2 \leftarrow \tilde{X}\ ^1A_1$ band system of the isotopomer $^{16}O_3$; r_{000} and θ_{000} values.
[e]Reference 18. Absorption spectra.
[f]Reference 13, T_0 value.
[g]Reference 19(b).
[h]Reference 19(a).
[i]This state can be considered as the local minimum of the two Renner–Teller components, $1\ ^3A'$ and $2\ ^3A''$.

180° through complete dissociation to O_2+O, optimizing at the same time the bond distances at every θ point in a C_{2v} fashion at the *ic*MRCI level. However, all calculations have been done under C_s constraints.

In all present calculations the correlation consistent polarized valence basis set of quadruple cardinality, cc-pVQZ $=12s6p3d2f1g$ was used, generally contracted to $[5s4p3d2f1g]$ $(=4Z)$.[15] For the O_3 molecule, this basis set creates a functional space of 165 spherical Gaussians. The zeroth order (CASSCF) wave function has been constructed by distributing the 18 valence electrons $[(2s^22p^4)\times 3]$ in 15 orbitals, 12 of a' and 3 of a'' symmetry species. Depending on the symmetry, CASSCF expansions range from about 8000 to 11 500 configuration functions (CF), with *ic*MRCI expansions from 5 to 8×10^6 CFs.

We report geometric and electronic features of O_3 for 13 states spanning an energy distance of 4 eV. All calculations were done with the MOLPRO suite of codes.[16]

II. RESULTS AND DISCUSSION

In what follows, Secs. II A–II D, we present details of PEPs of similar symmetry, namely, $(1,2)\ ^1A'$, $(1,2)\ ^1A''$, $(1,2)\ ^3A'$, and $(1,2)\ ^3A''$. Table I lists pertinent numerical results of 13 states, whereas Fig. 1 displays all calculated PEPs, and Figs. 2–5 PEPs of the same C_s symmetry. We remind that all calculations were performed at the *ic*MRCI/4Z level; no corrections of any kind, i.e., core electrons $(\sim 1s^2)$, basis set superposition errors, or scalar relativistic effects were taken into account, deemed of minor im-

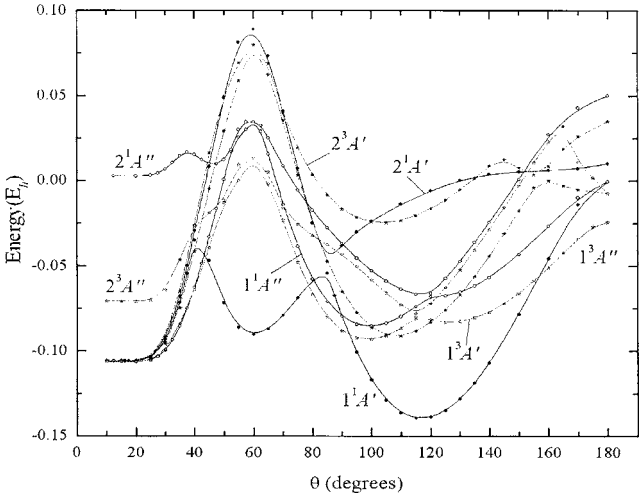

FIG. 1. MRCI/4Z PEPs of (1,2) $^1A'$, (1,2) $^1A''$, (1,2) $^3A'$, and (1,2) $^3A''$ symmetries.

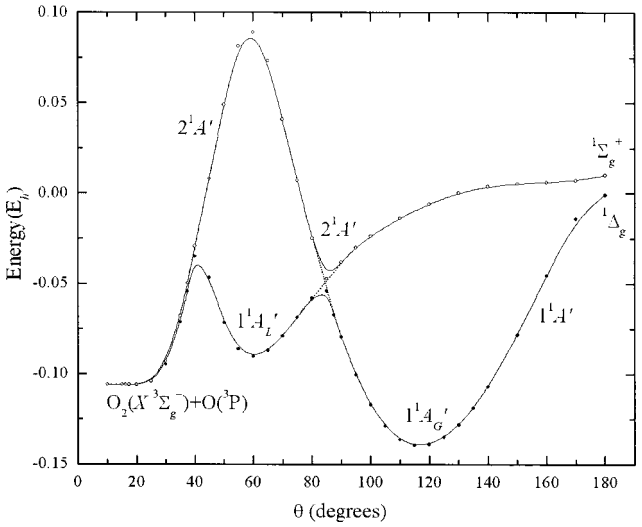

FIG. 2. MRCI/4Z PEPs of (1,2) $^1A'$ symmetries.

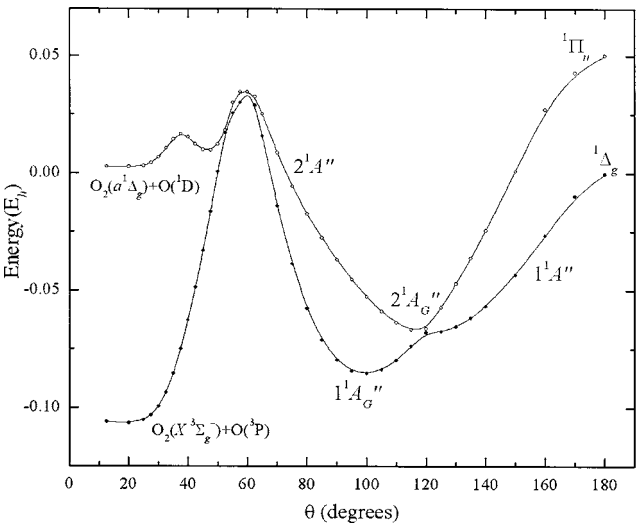

FIG. 3. MRCI/4Z PEPs of (1,2) $^1A''$ symmetries.

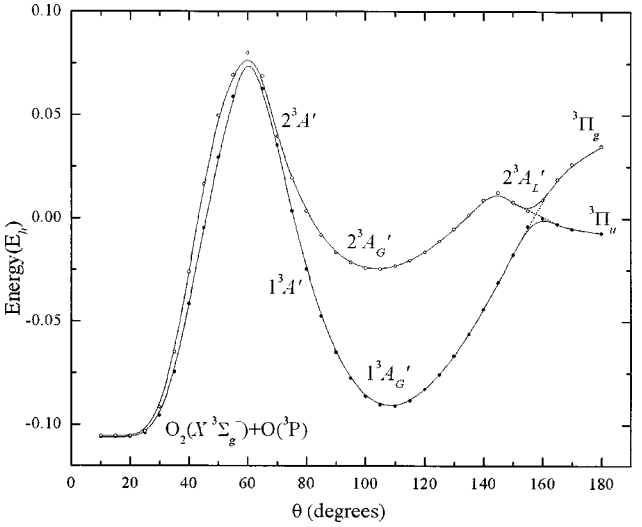

FIG. 4. MRCI/4Z PEPs of (1,2) $^3A'$ symmetries.

portance within the scope of the present work. Size nonextensivity errors are mitigated through the Davidson correction for unlinked clusters (+Q). In all calculations the O_3 molecule lies on the yz plane, the z axis being defined by the internuclear line O(1)–O(2) with the O(1) atom located at the origin.

A. 1 $^1A'$ and 2 $^1A'$

The ground state of O_3 is of $^1A'$ (C_s) symmetry, or $^1A_1$ in the C_{2v} point group, determined as global (G) minimum on the $^1A'$ curve and denoted as $\tilde{X}\ ^1A_G'$ in Table I. The calculated geometry (r_e, θ_e) and dipole moment (μ_e) are in excellent agreement with the experimental values. With respect to $O_2(X\ ^3\Sigma_g^-)+O(^3P)$ our D_e at the MRCI(+Q) level is 22.71 (23.3) kcal/mol; this should be contrasted with the experimental number $D_e=26.105\pm0.392$ kcal/mol.[20] For comparison, we give the best theoretical values so far at the MRCI level (MRCI/cc-pV5Z level) [Ref. 7(f)] $r_e=1.271$ Å, $\theta_e=116.9°$, and $D_e=23.8$ kcal/mol, practically identical to ours. The same authors give a D_e value obtained at the

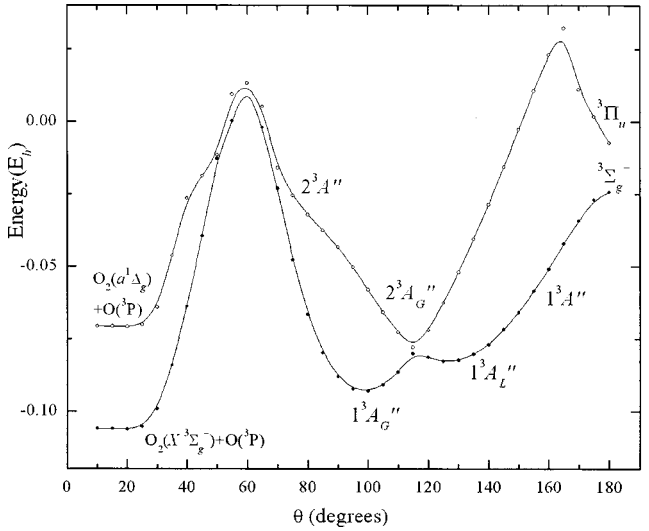

FIG. 5. MRCI/4Z PEPs of (1,2) $^3A''$ symmetries.

multireference average quadratic coupled cluster, MR-AQCC/cc-pV5Z level, but the results cannot be considered as reliable judging from the last two columns of Table IV of Ref. 7(f). Finally, our calculated harmonic frequencies, $\omega_1(ss;a_1)=1140.8$, $\omega_2(b;a_1)=718.6$, and $\omega_3(as;b_2)=1102.5\ \mathrm{cm}^{-1}$, are in very good agreement with the corresponding experimental values,[21] 1134.9, 716.0, and 1089.2 cm^{-1}.

The leading CASSCF configurations for the $\tilde{X}\ ^1A'_G$ state are as follows:

$$
\begin{aligned}
|\tilde{X}\ ^1A'_G\rangle &\approx 0.91|1a'^2 2a'^2 3a'^2 4a'^2 5a'^2 6a'^2 7a'^2 8a'^2 9a'^2 10a'^2 1a''^2 2a''^2\rangle \\
&\quad - 0.29|1a'^2 2a'^2 3a'^2 4a'^2 5a'^2 6a'^2 7a'^2 8a'^2 9a'^2 10a'^2 1a''^2 3a''^2\rangle \\
&= |7a'^2 8a'^2 9a'^2 10a'^2[(0.91)1a''^2 2a''^2 - (0.29)1a''^2 3a''^2]\rangle,
\end{aligned}
$$

suppressing finally the first six a' orbitals, which are, in essence, linear combinations of the $1s^2$ and $2s^2$ atomic oxygen orbitals. Notice that the a' and a'' orbitals lie on the molecular plane (yz) and along the x axis, respectively.

The configurations above point clearly to a closed shell (regular) singlet; the "0.29" component is a usual $2a''^2 \rightarrow 3a''^2$ excitation, or in a slightly different language, a GVB correlation. As the $\measuredangle \mathrm{OOO}(=\theta)$ angle increases from θ_e to $\theta=180°$, the 0.29 component diminishes monotonically until it reaches a value of "0.15" at the linear arrangement $^1\Delta_g$. In the linear configuration the O_3 molecule is described adequately by two configurations of equal weight,

$$
\begin{aligned}
|^1\Delta_g(^1A')\rangle &\approx 0.66(|7a'^2 8a'^2 9a'^2 1a''^2 2a''^2 3a''^2\rangle \\
&\quad - |7a'^2 8a'^2 9a'^2 10a'^2 1a''^2 2a''^2\rangle).
\end{aligned}
$$

The only way that a lowest $^1\Delta_g$ symmetry can be realized is through the interaction of $O_2(a\ ^1\Delta_g)+O(^1\mathrm{D};M_L=0) \rightarrow O_3(^1\Delta_g)$. Using valence-bond-Lewis (vbL) diagrams we have the following bonding scheme

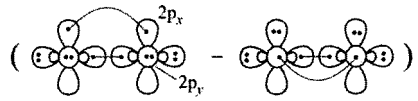

$O_2(a^1\Delta_g)$

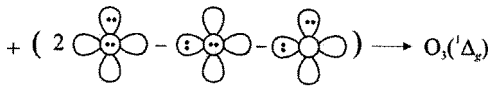

$O(^1\mathrm{D};M_L=0)$

We recall that $a\ ^1\Delta_g$ and ^1D are the first excited states of O_2 and O, located experimentally (theoretically) 22.64 (22.37) and 45.15 (45.82) kcal/mol above the $X\ ^3\Sigma_g^-$ and ^3P states, respectively.[22,23]

The bond distance and energy of the $^1\Delta_g$ linear configuration are $r=1.308$ Å and $E=-225.000\ 59\ E_h$.

The smooth correlation of the $\tilde{X}\ ^1A'_G$ state to the $^1\Delta_g$ linear configuration suggests that the ground state of ozone is formed from $O_2(a\ ^1\Delta_g)$ and $O(^1D)$. The linear attack of $O(^1D)$ to $O_2(a\ ^1\Delta_g)$ gives rise to $^1\Delta_g$ O_3 symmetry, whereas a perpendicular one leads to the $\tilde{X}\ ^1A'_G$ state, the bent structure being more stable, obviously because the p_π electrons of O_2 are easily accessible as compared to the σ ones along the z axis.

The upshot of this discussion is that the ground state of O_3 is a genuine *closed shell* singlet formed from $O_2(a\ ^1\Delta_g)$ and $O(^1D)$, or that one of the *in situ* oxygen atoms is in its first excited ^1D state, and the remaining *in situ* O_2 in the $a\ ^1\Delta_g$ state. This is shown schematically by the vbL diagram given below

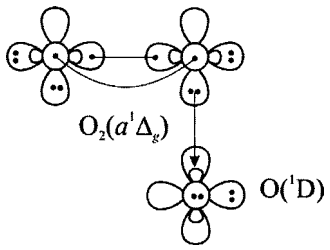

This diagram rationalizes the bent structure of O_3 and the positively charged, +0.24 at the CASSCF or MRCI/4Z level, of the central atom. Following a more conventional chemical language the previous diagram can be written as

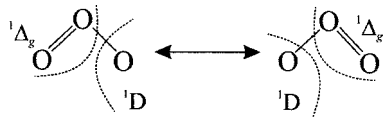

in conformity with the traditional "bonding" textbook icons.[2,24] This picture explains as well the low adiabatic dissociation energy of O_3 with respect to $O_2(X\ ^3\Sigma_g^-)+O(^3P)$, $D_e=26.1$ kcal/mol.[20] However, with respect to $O_2(a\ ^1\Delta_g)+O(^1D)$ the experimental (theoretical, MRCI+Q) binding energy is $D_e=26.1+22.64(a\ ^1\Delta_g \leftarrow X\ ^3\Sigma_g^-)^{22}+45.15(^1D \leftarrow {}^3P)^{23}$ kcal/mol=93.9(91.9) kcal/mol, a much more "reasonable" value. In comparison, the binding energy of $O_2(X\ ^3\Sigma_g^-)$ is $D_e=120.2$ kcal/mol.[22]

Moving now further to the left of the $1\ ^1A'$ curve and after passing a barrier of 55.2 kcal/mol due to the avoided crossing between the $1\ ^1A'$ and $2\ ^1A'$ curves at $\theta=85°$ (Fig. 2), the ozone molecule is trapped in a local (L) minimum with D_{3h} geometry $(1\ ^1A'_L)$. This equilateral cyclic isomer of O_3 has not been observed experimentally, but it has been extensively studied theoretically.[5(b),25–27,7(f),28,29] The

best theoretical numbers so far are those of Ref. 7(f) at the MRCI/cc–pV5Z level: $r_e=1.438$ Å and $T_e=10\,912.4$ cm^{-1}, in very good agreement with the results of the present work (Table I). With respect to $O_2(X\,^3\Sigma_g^-)+O(^3P)$, the $1\,^1A_L'$ state is unbound by 8.45 (7.5) kcal/mol. Our three calculated harmonic frequencies (two degenerate) are $\omega_{1,2}=794.1$ and $\omega_3=1115.1$ cm^{-1}, as compared to the calculated vibrational energy differences $\Delta G(01\leftarrow 00)=790.8$ cm^{-1} and $\Delta G(10\leftarrow 00)=1088.4$ cm^{-1} of Qu *et al.*[29]

The main CASSCF $1\,^1A_L'$ configuration and Mulliken atomic populations are $|1\,^1A_L'\rangle \approx 0.93|7a'^2 8a'^2 9a'^2 1a''^2 2a''^2 3a''^2\rangle$ and $2s^{1.92}2p_x^{1.98}2p_y^{1.03}2p_z^{0.99}3d^{0.06}$, identical for all three atoms by symmetry. Obviously, the *in situ* atoms are in their ground ^3P state with the bonding clearly pictured by the vbL diagram

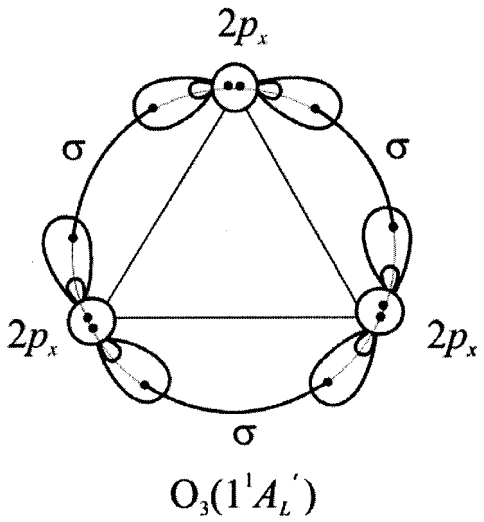

The instability of the $1\,^1A_L'$ isomer is due to the nonoptimum direction of the $2p_y$ and $2p_z$ atomic orbitals leading to a small overlap and the Coulomb–Pauli repulsion of the three $2p_x$ electron pairs perpendicular to the molecular plane (yz). This "strained" cyclic configuration reminds the cyclopropane molecule (C_3H_6) isoelectronic to O_3. The oxygen atom is isoelectronic to the parent carbine $CH_2(\tilde{X}\,^3B_1)$; its ground state being also of $^3B_1$ symmetry under C_{2v} constraints. It is remarkable that by bringing together in a proper fashion three CH_2 species in their $\tilde{X}\,^3B_1$ state, the highly strained cyclopropane molecule is obtained. Cyclopropane, although highly strained, is quite stable with a boiling point of −32.9 °C and a melting point of −127 °C, and a topology identical to that of the cyclic ozone, from which the former is obtained upon substitution of the six p_π electrons by six $H(^2S)$ atoms distributed above and below the planar skeleton.

The $2\,^1A'$ PEP correlates to the $^1\Sigma_g^+$ structure ($\theta=180°$), 6.8 (7.3) kcal/mol higher than the corresponding linear $^1\Delta_g(1\,^1A')$ arrangement. At $\theta=85°$ and $r_e=1.3924$ Å we have a minimum ($^1A_1$), the result of an avoided crossing between the $1\,^1A'$ and $2\,^1A'$ profiles; see Table I and Fig. 2. The barrier to linearity ($^1\Sigma_g^+$) is BL=36.0 kcal/mol, whereas the barrier to dissociation, from $\theta=85°$ to $\theta=60°$, is 85.6 kcal/mol. The same avoided crossing has been previously discussed by Banichevich and Peyerimhoff.[6(e)] However, their numerical results are considerably different from ours ($\theta=87°$, $r_e=1.46$ Å, $T_e=20\,164$ cm^{-1}), mainly due to the size of their basis set. The leading CASSCF configurations of the $2\,^1A'$ state is $|2\,^1A'\rangle \approx |[(0.87)7a'^2 8a'^2 9a'^2 - (0.33)7a'^2 8a'^2 10a'^2]1a''^2 2a''^2 3a''^2\rangle$, similar to the character of the cyclic $1\,^1A_L'$ state, and with practically identical Mulliken populations, mirroring the *in situ* ^3P ground state of the oxygen atoms.

B. $1\,^1A''$ and $2\,^1A''$

The $1\,^1A''$ PEP is the second Renner–Teller companion of the $^1\Delta_g$ linear configuration, the first one being the $1\,^1A'$ previously discussed: Figs. 1 and 3. As the ∢OOO angle decreases the $1\,^1A''$ curve suffers an avoided crossing at $\theta=120°$ with the $2\,^1A''$; the latter correlates to the linear structure $^1\Pi_u$. Under C_{2v} restrictions the $1\,^1A''$ and $2\,^1A''$ cross each other at $\theta=120°$, belonging to the symmetry species $^1B_1$ and $^1A_2$, respectively.[6(c),7(c)] The $1\,^1A''$ correlates to the ground state fragments $O_2(X\,^3\Sigma_g^-)+O(^3P)$, it is unbound with respect to these products by 13.1 kcal/mol and has an energy barrier of 75.1 kcal/mol at $\theta=60°$.

The first experimental measurement on the low-lying excited states of O_3 was published in 1990 by Anderson *et al.*[30] These workers reported that $T_e(1\,^1A''(^1A_2)\leftarrow\tilde{X}\,^1A_G'(^1A_1))=9990\pm 70$ cm^{-1}, $\omega_1(ss)\approx 1200$ cm^{-1}, $\omega_2(b)=528\pm 15$ cm^{-1}, and $\omega_3(as)\approx 90\pm 80$ cm^{-1}. A few years later Arnold *et al.*[13] through anion photoelectron spectroscopy obtained $T_0\approx 12\,905$ cm^{-1} and $\omega_2(b)=690\pm 100$ cm^{-1}. Our T_e MRCI(+Q) value is 12 514(11 972) cm^{-1}, with $\omega_1(ss)=1085.8$ cm^{-1} and $\omega_2(b)=557.2$ cm^{-1}. However, our asymmetric stretching frequency $\omega_3(as)$ is imaginary, i.e., $\omega_3(as)=223i$ cm^{-1}. As far as we know the ω_3 frequency has never been calculated before, but it has been stated as early as 1991 that it is imaginary.[31] Our MRCI(+Q) r_e and θ_e values, Table I, are in perfect agreement with the recent ones calculated by Grebenshchinkov *et al.*[8,32]

The main equilibrium CASSCF CFs of the $1\,^1A''$ state are

$$|1\,^1A''\rangle \approx |7a'^2 8a'^2 9a'^2 1a''^2 2a''^2[0.62(10\bar{a}'^1 3a''^1 - 10a'^1 3\bar{a}''^1)]\rangle + |7a'^2 8a'^2 10a'^2 1a''^2 3a''^2[0.27(9a'^1 2\bar{a}''^1 - 9\bar{a}'^1 2a''^1)]\rangle$$

clearly an *open shell singlet*. As was already mentioned, the $1\,^1A''$ state correlates to the linear $^1\Delta_g$ configuration whose CASSCF CFs are very similar to the ones of the bent state, simply the "0.62" and "0.27" coefficients become "0.65" and "0.15," respectively.

The $2\,^1A''$ PEP, or $^1B_1$ under C_{2v} restrictions, presents a global and a local minimum at $\theta=120.1°$ ($2\,^1A_G''$) and $\theta=46.43°$ ($2\,^1A_L''$): see Fig. 3. At the MRCI(+Q) level we obtain $r_e=1.3504(1.353)$ Å, $\theta_e=120.1(118.0)°$, and $T_e(2\,^1A_G''\leftarrow\tilde{X}\,^1A_G')=16\,669.3(15\,966)$ cm^{-1}, as contrasted to the experimental T_e value of $16\,385\pm 20$ cm^{-1} [Ref. 19(a)] or $16\,454\pm 242$ cm^{-1}.[19(b)] The corresponding numbers of

Grebenshchinkov *et al.*[8] are $r_e=1.3346$ Å, $\theta_e=121.38°$, and $T_e=15\,776$ cm^{-1}. Although two of the experimental frequencies are known,[19(a)] namely, $\omega_1=1213\pm5$ cm^{-1} and $\omega_2=638\pm5$ cm^{-1}, we were unable to calculate them as our minimum sits on an avoided crossing because of the C_s symmetry presently used. Under C_{2v} constraints the two curves 1 $^1A''$ and 2 $^1A''$ transform to "quasidiabatic" $^1A_2$ and $^1B_1$ and cross each other. The calculated frequencies of the 2 $^1A''(^1B_1)$ state at the MRCI/aug-cc-pVQZ level given in Ref. 8 are $\omega_1(ss)=920$ cm^{-1}, $\omega_2(b)=560$ cm^{-1}, and $\omega_3(as)=1020$ cm^{-1}, differing considerably from the experimental ones.[19(a)]

The leading CASSCF CFs of the 2 $^1A''_G$ state and its corresponding linear companion $^1\Pi_u$ are as follows:

$$|2\,^1A''_G\rangle \approx 0.60|7a'^2 8a'^2 10a'^2 1a''^2 2a''^2 (9\bar{a}'^1 3a''^1 - 9a'^1 3\bar{a}''^1)\rangle + 0.31|7a'^2 8a'^2 9a'^2 1a''^2 3a''^2 (10a'^1 2\bar{a}''^1 - 10\bar{a}'^1 2a''^1) 3a''^2\rangle,$$

$$|^1\Pi_u\rangle \approx 0.59|7a'^2 8a'^2 9a'^2 1a''^2 2a''^2 (11\bar{a}'^1 3a''^1 - 11a'^1 3\bar{a}''^1)\rangle - 0.19|7a'^2 8a'^2 10a'^2 1a''^2 2a''^2 (11\bar{a}'^1 3a''^1 - 11a'^1 3\bar{a}''^1)\rangle,$$

with no doubt open singlets.

With respect to the adiabatic species $O_2(a\,^1\Delta_g)+O(^1D)$ the binding energy of 2 $^1A''_G$ is $D_e=43.24$ kcal/mol, but it is unbound with respect to $O_2(X\,^3\Sigma_g^-)+O(^3P)$ by 24.35 kcal/mol.

On the 2 $^1A''$ PEP a shallow local minimum is observed (2 $^1A''_L$) at $\theta=46.43°$ and $r_e=1.720$ Å, with a barrier to dissociation of 5.45 kcal/mol (Fig. 3). With respect to the $O_2(a\,^1\Delta_g)+O(^1D)$ fragments this "state" is higher by 3.3 kcal/mol. The 2 $^1A''_L$ minimum has also been located by Xantheas *et al.*[31] at the CASSCF level.

C. 1 $^3A'$ and 2 $^3A'$

The PEPs of the 1 $^3A'$ and 2 $^3A'$ are displayed in Fig. 4. Under C_s symmetry the global minimum of the 1 $^3A'$ curve (1 $^3A'_G$) correlates to a linear $^3\Pi_u$ configuration due to an avoided crossing at near 160° with the 2 $^3A'$ PEP. In other words, *diabatically*, the 1 $^3A'_G$ traces its ancestry to the $^3\Pi_g$ linear arrangement, whereas the $^3\Pi_u$ is inherently of repulsive nature.

The only experimental findings for the 1 $^3A'_G$ ($^3B_2$ under C_{2v}) are the $T_0(1\,^3A'_G \leftarrow \tilde{X}\,^1A'_G)=10\,485$ cm^{-1} and $\omega_2(b)=580\pm50$ cm^{-1} (Ref. 13); a second T value of $10\,405\pm242$ cm^{-1} is given in Ref. 19(b). At the MRCI(+Q) level we obtain $T_e=11\,063(10\,793)$ cm^{-1}, $r_e=1.3542(1.355)$ Å, and $\theta_e=108.55(108.47)°$; see Table I. Similar geometrical results have been reported in Ref. 7(e) at the CASPT2/4s3p2d1f level, and the MRCI/cc-pVQZ.[33] With respect to $O_2(X\,^3\Sigma_g^-)+O(^3P)$ the 1 $^3A'_G$ state is unbound by 9.0 kcal/mol, but the energy barrier to dissociation with respect to θ is 107.7 kcal/mol. However, we were unable to calculate the three harmonic frequencies due to severe technical problems. At $\theta=60°$ the two curves 1 $^3A'$ and 2 $^3A'$ are degenerate, marking a conical intersection.

The most significant configuration is

$$|1\,^3A'_G(^3B_2)\rangle \approx 0.96|7a'^2 8a'^2 9a'^2 10a'^2 1a''^2 2a''^1 3a''^1\rangle,$$

with $1a'' \approx 0.83(2p_{x(2)}) + 0.29(2p_{x(1)} + 2p_{x(3)})$, $2a'' \approx 0.60(2p_{x(2)}) - 0.66(2p_{x(1)} + 2p_{x(3)})$ and $3a'' \approx 0.72(2p_{x(1)} - 2p_{x(3)})$. In accord also with the CASSCF Mulliken atomic populations, the bonding can be represented by the following vbL graph

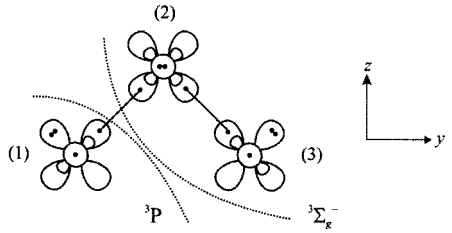

Note that the *in situ* oxygen atoms are in their ^3P ground state with the two uncoupled electrons distributed perpendicularly to the molecular plane. Alternatively, an *in situ* O_2 (O_2-O_3 or O_1-O_2) is in the $X\,^3\Sigma_g^-$ state with the third oxygen (O_1 or O_3) in the ^3P state.

The shallow minimum of the 2 $^3A'$ at $\theta=155°$ results from the avoided crossing between the 1 $^3A'$ and 2 $^3A'$ PEPs under C_s symmetry. A second avoided crossing occurs with an incoming (not calculated) 3 $^3A'$ curve that transfers its character to the 2 $^3A'_G(^3B_2)$ state; see Fig. 4. The MRCI(+Q) molecular parameters are $T_e(2\,^3A'_G \leftarrow \tilde{X}\,^1A'_G)=25\,322.3(25\,158)$ cm^{-1}, $r_e=1.4234(1.424)$ Å, and $\theta_e=103.7(103.7)°$. The leading configuration is

$$|2\,^3A'_G(^3B_2)\rangle \approx 0.95|7a'^2 8a'^2 9a'^1 10a'^1 1a''^2 2a''^2 3a''^2\rangle,$$

with $9a' \approx 0.73(2p_{y(1)} + 2p_{z(3)})$ and $10a' \approx 0.67(2p_{y(1)}) - 0.60(2p_{z(3)}) + 0.35(2p_{y(3)})$. The CASSCF atomic Mulliken densities are identical to those of the 1 $^1A'_L$ (cyclic isomer), indicative of the ground state ^3P *in situ* character of the three oxygen atoms. The emerging bonding picture is given below

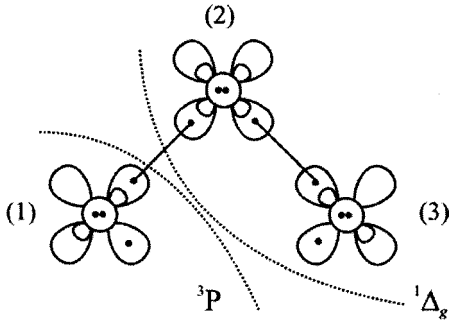

the same with the previous one but with the singly occupied $2p$ orbitals lying on the molecular plane (yz). Clearly, coupling the singly occupied orbitals into a singlet, the cyclic isomer 1 $^1A'_L$ obtains (*vide supra*). It is also interesting to notice that an *in situ* O_2 (O_2-O_3 or O_1-O_2) molecule is in the $a\,^1\Delta_g$ electronic configuration, the third oxygen (O_1 or O_3) atom being in the ^3P state.

D. 1 $^3A''$ and 2 $^3A''$

Figure 5 shows the 1 $^3A''$ and 2 $^3A''$ PEPs which suffer an avoided crossing at $\theta=117°$. At $\theta=180°$ the 1 $^3A''$ curve becomes $^3\Sigma_g^-$ represented adequately by the leading CASSCF configuration, $|^3\Sigma_g^-\rangle \approx 0.93|7a'^2 8a'^2 9a'^2 10a'^1 1a''^2 2a''^2 3a''^1\rangle$. Upon bending we meet the first (local) minimum 1 $^3A_L''$ (or $^3B_1$ under C_{2v}) at $\theta=126.44°$, whose main configuration is identical with that of the linear $^3\Sigma_g^-$ arrangement but with a variational leading coefficient of "0.90." The vbL diagram below captures the bonding nature of the 1 $^3A_L''(^3B_1)$ state, supported also by the CASSCF Mulliken atomic populations

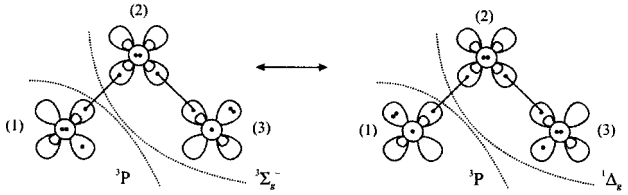

Observe that all three oxygen atoms are in the ground ^3P state with the singly occupied $2p$ orbitals perpendicular to each other. Alternatively, we can consider the 1 $^3A_L''$ state of O_3 molecule as a "resonance" structure of an *in situ* $O_2(^1\Delta_g)+O(^3P)$ and $O_2(^3\Sigma_g^-)+O(^3P)$. It should be noted that the electronic structure of this state is of the same type with that of the 1 $^1A''$ previously discussed, but with the two $2p$ electrons of the latter coupled into a singlet. This is the reason that these states are practically degenerate, differing by $1.5mE_h$, the singlet being lower; see Table I. From Table I we can see that our calculated $T_e(1\ ^3A_L'' \leftarrow \tilde{X}\ ^1A_G')$ separation is in a very good agreement with the corresponding experimental values.[13,19]

The global minimum of the 1 $^3A''$ curve, 1 $^3A_G''$ (or $^3A_2$ under C_{2v}), results from an avoided crossing with the 2 $^3A''$ curve near $\theta=117°$; the latter has already suffered an avoided crossing at about 165° with another (not calculated) PEP of the same symmetry. The main CASSCF CFs of the 1 $^3A_G''$ state are

$$|1\ ^3A_G''\rangle \approx 0.89|7a'^2 8a'^2 9a'^2 10a'^1 1a''^2 2a''^2 3a''^1\rangle + 0.33|7a'^2 8a'^2 9a'^1 10a'^2 1a''^2 2a''^1 3a''^2\rangle,$$

not very different from those of the local minimum 1 $^3A_L''$. As a result the bonding is of the same nature as in the 1 $^3A_L''(^3B_1)$, but its structural characteristics are dissimilar. At the MRCI(+Q) level we obtain $r_e=1.3412(1.342)$ Å, $\theta_e=98.78(98.6)°$, and $T_e(1\ ^3A_G'' \leftarrow \tilde{X}\ ^1A_G')=10\ 643(9968)$ cm^{-1}. Corresponding experimental numbers are $r_e=1.345$ Å, $\theta_e=98.9°$,[17] and $T_e=9963\pm4$ cm^{-1},[18] in excellent agreement with the present values. With respect to $O_2(X\ ^3\Sigma_g^-)+O(^3P)$, the 1 $^3A_G''$ state is unbound by 7.78 (4.9) kcal/mol and has an energy barrier to dissociation with respect to the θ coordinate of 67.07 (65.71) kcal/mol. At 60° the two PEPs, 1 $^3A''$ and 2 $^3A''$, show a Jahn–Teller degeneracy; see Fig. 5.

The 2 $^3A''$ curve correlates to the linear $^3\Pi_u$ state; as the molecule is bent ($^3B_1$) the energy raises up to 165° where it meets a third $^3A''$ curve. Subsequently, the energy plummets along a $^3A_2$ branch ending to a minimum at 115°. The rest of the 2 $^3A''$ curve follows a $^3B_1$ path until a maximum at 60° when it becomes degenerate with the 1 $^3A''$ PEP. Numerical values of the global minimum 2 $^3A_G''$, the local being the linear configuration, are presented in Table I.

III. SUMMARY AND REMARKS

The present study examines the electronic structure of a few low-lying states of the ozone molecule, namely, $\tilde{X}\ ^1A_G'(\tilde{X}\ ^1A_1)$, $1\ ^3A_G''(^3A_2)$, $1\ ^1A_L'(^1A_1)$, $1\ ^3A_G'(^3B_2)$, $1\ ^1A''(^1A_2)$, $1\ ^3A_L''(^3B_1)$, $2\ ^3A_G''$, $2\ ^1A_G''$, $2\ ^1A'(^1A_1)$, $2\ ^3A_G'(^3B_2)$, $^3\Pi_u$, $2\ ^3A_L'$, and $2\ ^1A_L''$, a total of 13 minima spanning an energy range of 4 eV. All calculations were performed at the valence MRCI (=CASSCF+1+2)/cc-pVQZ level of theory under general C_s symmetry conditions. We have constructed PEPs along the bending coordinate from 180° to dissociation products $O_2(X\ ^3\Sigma_g^-$ or $a\ ^1\Delta_g)+O(^3P$ or $^1D)$, optimizing at the same time the O–O–O distance(s) in a symmetrical fashion. The 13 states presently studied were found as global (G) or local (L) minima on the constructed PEPs. All our numerical results are in very good agreement with available experimental values.

The focus of this work is the critical examination of the structure and bonding of certain low-lying states, some of which are studied systematically and at this level for the first time.

For the ground $\tilde{X}\ ^1A_G'(\tilde{X}\ ^1A_1)$ state, the analysis of our results indicates clearly that it is a regular singlet, not an open singlet as it was accepted up to now, with all the *in situ* oxygen atoms in their ground ^3P state. Our results consistently support that the bonding in the X state is formed from the first excited states of $O_2(a\ ^1\Delta_g)$ and $O(^1D)$ through a perpendicular attack of the latter to a p_π electron pair of O_2. In the elusive cyclic isomer, 1 $^1A_L'(^1A_1)$, the *in situ* oxygen atoms are in the ground ^3P state with the three $2p$ oxygen electron pairs perpendicular to the molecular plane. An interesting similarity of the 1 $^1A_L'$ state is noticed with the isoelectronic highly strained but stable molecule cyclopropane $[C_3H_6=(CH_2)_3]$.

In the states 1 $^3A_G'(^3B_2)$ and 2 $^3A_G'(^3B_2)$ the three *in situ* oxygen atoms are in the ^3P state, with the two unpaired electrons perpendicular and parallel to the molecular plane, respectively. In other words an *in situ* O_2 finds itself in the $^3\Sigma_g^-$ state (1 $^3A_G'$) and in the $^1\Delta_g$ state 2 $^3A_G'$.

The bonding in the 1 $^3A_G''(^3A_2)$ and 1 $^3A_L''(^3B_1)$ states is similar and indeed intriguing. All three oxygen atoms are also in their ground ^3P states, but the unpaired electrons are perpendicular to each other. Alternatively, the molecule can be thought of as a resonance of the *in situ* species $[O_2(^3\Sigma_g^-)+O(^3P)] \leftrightarrow [O_2(^1\Delta_g)+O(^3P)]$.

Finally, calculated dipole moments range from 0.024 to 0.617 D, most of them obtained for the first time. Based on the very good agreement between experiment and theory for the $\tilde{X}\ ^1A_G'$ state, 0.5337 vs 0.546 D, we strongly believe that the values of all calculated dipole moments should be close to reality.

[1] Vl. G. Tyuterev, S. Tashkun, P. Jensen, A. Barbe, and T. Cours, J. Mol. Spectrosc. **198**, 57 (1999).
[2] R. Trambarulo, S. N. Ghosh, C. A. Burrus, Jr., and W. Gordy, J. Chem. Phys. **21**, 851 (1953).

[3] K. M. Mack and J. S. Muentir, J. Chem. Phys. **66**, 5278 (1977).
[4] M. J. Molina and F. S. Rowland, Nature (London) **249**, 810 (1974).
[5] (a) P. J. Hay and W. A. Goddard III, Chem. Phys. Lett. **14**, 46 (1972); (b) W. A. Goddard III, T. H. Dunning, Jr., W. J. Hunt, and P. J. Hay, Acc. Chem. Res. **6**, 368 (1973); (c) P. J. Hay, T. H. Dunning, Jr., and W. A. Goddard III, Chem. Phys. Lett. **23**, 457 (1973); (d) P. J. Hay, T. H. Dunning, Jr., and W. A. Goddard III, J. Chem. Phys. **62**, 3912 (1975); (e) P. J. Hay and T. H. Dunning, Jr., *ibid.* **67**, 2290 (1977).
[6] (a) K.-H. Thunemann, S. D. Peyerimhoff, and R. J. Buenker, J. Mol. Spectrosc. **70**, 432 (1978); (b) A. Banichevich, S. D. Peyerimhoff, and F. Grein, Chem. Phys. Lett. **173**, 1 (1990); (c) A. Banichevich, S. D. Peyerimhoff, J. A. Beswick, and O. Atabek, J. Chem. Phys. **96**, 6580 (1992); (d) A. Banichevich, S. D. Peyerimhoff, and F. Grein, Chem. Lett. **195**, 459 (1992); (e) A. Banichevich and S. D. Peyerimhoff, Chem. Phys. Lett. **174**, 93 (1993); (f) A. Banichevich and S. D. Peyerimhoff, Chem. Phys. **178**, 155 (1993).
[7] (a) C. W. Wilson, Jr. and D. G. Hopper, J. Chem. Phys. **74**, 595 (1981); (b) W. D. Laidig and H. F. Schaefer III, *ibid.* **74**, 3411 (1981); (c) M. Braunstein, P. J. Hay, R. L. Martin, and R. T. Pack, *ibid.* **95**, 8239 (1991); (d) M. Braunstein and R. T. Pack, *ibid.* **96**, 6378 (1992); (e) P. Borowski, M. Fulscher, P.-Å. Malmqvist, and B. O. Roos, Chem. Phys. Lett. **237**, 195 (1995); (f) T. Müller, S. S. Xantheas, H. Dachsel, R. J. Harrison, J. Nieplocha, R. Shepard, G. S. Kedziora, and H. Lischka, *ibid.* **293**, 72 (1998); (g) D. Xie, H. Guo, and K. A. Peterson, J. Chem. Phys. **112**, 8378 (2000); (h) D. Xie, H. Guo, and K. A. Peterson, *ibid.* **115**, 10404 (2001); (i) O. Hino, T. Kinoshita, G. K.-L. Chan, and R. J. Bartlett, *ibid.* **124**, 114311 (2006).
[8] S. Yu. Grebenshchikov, Z.-W. Qu, H. Zhu, and R. Schinke, Phys. Chem. Chem. Phys. **9**, 2044 (2007), and references therein.
[9] R. J. Blint and M. D. Newton, J. Chem. Phys. **59**, 6220 (1973).
[10] S. M. Adler−Golden, S. R. Langhoff, C. W. Bauschlicher, Jr., and G. D. Carney, J. Chem. Phys. **83**, 255 (1985).
[11] J. F. Stanton, R. J. Bartlett, D. H. Magers, and W. N. Lipscomb, Chem. Phys. Lett. **163**, 333 (1989).
[12] C. Meredith, G. E. Quelch, and H. F. Schaefer III, J. Am. Chem. Soc. **113**, 1186 (1991).
[13] D. W. Arnold, C. Xu, E. H. Kim, and D. M. Neumark, J. Chem. Phys. **101**, 912 (1994).
[14] C. Woywod, M. Stergle, W. Domcke, H. Flöthmann, and R. Schinke, J. Chem. Phys. **107**, 7282 (1997).
[15] T. H. Dunning, Jr., J. Chem. Phys. **90**, 1007 (1989); Basis sets were obtained from the Extensible Computational Chemistry Environment Basis Set Database, Version 02/02/06, as developed and distributed by the Molecular Science Computing Facility, Environmental and Molecular Sciences Laboratory which is part of the Pacific Northwest Laboratory, P.O. Box 999, Richland, Washington 99352, USA, and funded by the U.S. Department of Energy. The Pacific Northwest Laboratory is a multiprogram laboratory operated by Battelle Memorial Institute for the U.S. Department of Energy under Contract No. DE−AC06−76RLO 1830. Contact Karen Schuchardt for further information.
[16] MOLPRO, a package of *ab initio* programs written by H.-J. Werner, P. J. Knowles, R. Lindh *et al.*
[17] A. J. Bouvier, D. Inard, V. Veyret, B. Bussery, R. Bacis, C. Churassy, J. Brion, J. Malicet, and R. H. Judge, J. Mol. Spectrosc. **190**, 189 (1998).
[18] J. Günther, S. M. Anderson, G. Hilpert, and K. Mauersberger, J. Chem. Phys. **108**, 5449 (1998).
[19] (a) S. M. Anderson, J. Maeder, and K. Mauersberger, J. Chem. Phys. **94**, 6351 (1991); (b) S. M. Anderson and K. Mauersberger, J. Geophys. Res. **100**, 3033 (1995).
[20] M. W. Chase, Jr., C. A. Davies, J. R. Downey, Jr., D. J. Frurip, R. A. McDonald, and A. N. Syverud, J. Phys. Chem. Ref. Data **14**, 1 (1985).
[21] A. Barbe, C. Secroun, and P. Jouve, J. Mol. Spectrosc. **49**, 171 (1974).
[22] K. P. Huber and G. Herzberg (data prepared by J. W. Gallagher and R. D. Johnson III) in *NIST Chemistry WebBook*, NIST Standard Reference Database No. 69, edited by P. J. Linstrom and W. G. Mallard (National Institute of Standards and Technology, Gaithersburg, MD, 2005); http://webbook.nist.gov
[23] Yu. Ralchenko, A. E. Kramida, J. Reader, and NIST ASD Team, NIST Atomic Spectra Database, Version 3.1.4. National Institute of Standards and Technology, Gaithersburg, MD, 2008 (http://physics.nist.gov/asd3).
[24] See, for instance, N. N. Greenwood and A. Earnshaw, *Chemistry of the Elements*, 2nd ed. (Butterworth-Heinemann, Washington, DC, 1997); L. F. Fieser and M. Fieser, *Advanced Organic Chemistry* (Reinhold, New York, 1961).
[25] S. Shih, R. J. Buenker, and S. D. Peyerimhoff, Chem. Phys. Lett. **28**, 463 (1974).
[26] L. B. Harding and W. A. Goddard III, J. Chem. Phys. **67**, 2377 (1977).
[27] T. J. Lee, Chem. Phys. Lett. **169**, 529 (1990).
[28] R. Elliott, R. Compton, R. Levis, and S. Matsika, J. Phys. Chem. A **109**, 11304 (2005).
[29] Z.-W. Qu, H. Zhu, and R. Schinke, J. Chem. Phys. **123**, 204324 (2005).
[30] S. M. Anderson, J. Morton, and K. Mauersberger, J. Chem. Phys. **93**, 3826 (1990).
[31] S. S. Xantheas, G. J. Atchity, S. T. Elbert, and K. Ruedenberg, J. Chem. Phys. **94**, 8054 (1991).
[32] S. Yu. Grebenshchikov, R. Schinke, Z.-W. Qu, and H. Zhu, J. Chem. Phys. **124**, 204313 (2006).
[33] S. F. Deppe, U. Wachsmuth, B. Abel, M. Bittererová, S. Y. Grebenshchikov, R. Siebert, and R. Schinke, J. Chem. Phys. **121**, 5191 (2004).